



Electrochemical formation of Sm–Ni alloy films in a molten LiCl–KCl–SmCl₃ system

Takahisa Iida, Toshiyuki Nohira, Yasuhiko Ito ^{*,1}

Department of Fundamental Energy Science, Graduate School of Energy Science, Kyoto University, Sakyo-ku, Kyoto 606-8501, Japan

Received 20 October 2000; received in revised form 12 February 2001

Abstract

The electrochemical formation of Sm–Ni alloys was investigated in a molten LiCl–KCl–SmCl₃ (0.5 mol%) system at 723 K. The cyclic voltammogram for a Mo electrode showed the reduction wave from Sm(III) to Sm(II) at 1.60 V (vs Li⁺/Li), but no reduction wave from Sm(II) to Sm metal. For a Ni electrode, small cathodic currents were observed at potentials more negative than 0.10 V, which indicated the formation of Sm–Ni alloy. The formation of an SmNi₂ phase was confirmed by XRD analysis of a sample prepared at 0.10 V for 72 h. The thickness of the SmNi₂ film was estimated to be approximately 100 nm. A much thicker SmNi₂ film (~20 μm) was obtained by cathodic galvanostatic electrolysis at 50 mA cm⁻² in a time period as short as 1 h. Since Li metal was codepositing during the electrolysis and the SmNi₂ film was rapidly formed, this electrochemical formation method was termed the ‘Li codeposition method’. The formed SmNi₂ film was changed to other alloy phases by anodic potentiostatic electrolysis. The formation potentials of SmNi₅, SmNi₃ and SmNi₂ were found to be 1.20, 0.65 and 0.29 V, respectively. © 2001 Elsevier Science Ltd. All rights reserved.

Keywords: LiCl–KCl; Molten salt; Sm–Ni alloy; Electrolysis; Li codeposition method

1. Introduction

Recently, rare earth–transition metal alloys have been attracting much research with their excellent magnetic, hydrogen absorbing and catalytic properties. In particular, several Sm–transition metal alloys, e.g. Sm₂Fe₁₇N₃, SmCo₅ and Sm₂Co₁₇, are well known as super permanent magnets [1]. If these alloys can be formed as films with arbitrary shapes and sizes, various applications will be possible, for instance this will contribute significantly to micro machine technology [2]. On the other hand, the molten salt electrochemical

process has been investigated as a new formation method of the rare earth–transition metal alloy films in the authors’ laboratory [3–6]. This process has the following advantages:

1. phases of the alloy films can be controlled by electrochemical parameters (e.g. potential, current density);
2. the alloy films can be formed even on a large and/or complex shaped substrate;
3. mass production is easy.

From this background, the authors have been conducting a series of formations of Sm–transition metal alloy films by the molten salt electrochemical process. This paper describes the results of electrochemical formation of various types of Sm–Ni alloys in a molten LiCl–KCl–SmCl₃ system. In the LiCl–KCl–SmCl₃ system, the Sm(III) ion is reported to be reduced to the

* Corresponding author. Tel.: +81-75-753-5827; fax: +81-75-753-5906.

E-mail address: y-ito@energy.kyoto-u.ac.jp (Y. Ito).

¹ ISE member.

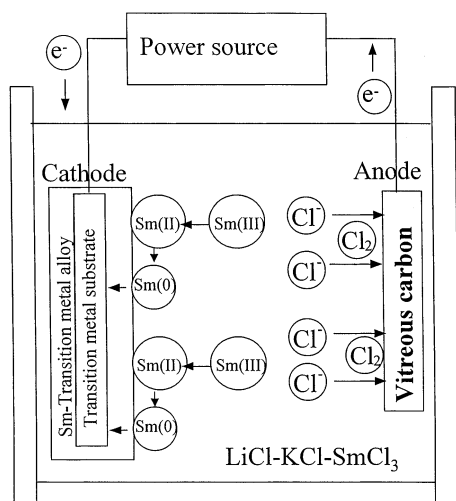


Fig. 1. Principle of the molten salt electrochemical process for Sm-transition metal alloy formation.

Sm(II) ion at about 1.60 V (vs Li^+/Li), and the reduction potential of the Sm(II) ion to Sm metal is thought to be more negative than the Li deposition potential [7]. However, electrochemical formation of Sm-transition metal alloys was expected because the alloy formation potential was thought to shift to a more positive potential than the elementary Sm deposition potential. Fig. 1 shows the principle of the molten salt electrochemical process for the expected Sm-transition metal alloy formation. When SmCl_3 is added to molten LiCl-KCl, SmCl_3 dissociates to form Sm(III) and Cl^- ions. By cathodic electrolysis, Sm(III) ions will be reduced to Sm(II) ions, and Sm(II) ions are expected to be reduced

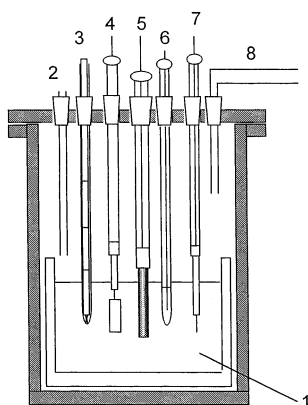


Fig. 2. Schematic drawing of the experimental apparatus. (1) LiCl-KCl-SmCl₃ (added 0.5 mol%), $T = 723$ K, (2) Ar gas inlet, (3) thermocouple, (4) working electrode (Mo or Ni), (5) counter electrode (vitreous carbon), (6) reference electrode (Ag^+/Ag), (7) Li^+/Li electrode (Ni wire) and (8) Ar gas outlet.

to Sm(0) to form Sm-transition metal alloys on a transition metal substrate.

2. Experimental

Fig. 2 shows the experimental apparatus. The LiCl-KCl eutectic (LiCl:KCl = 58.5:41.5 mol%; reagent grade, Wako Pure Chemical Co., Ltd.) was contained in a high purity alumina crucible (99.5 wt.% Al_2O_3 ; SSA-S grade, Nikkato Co., Ltd.) and dried under vacuum for more than 72 h at 473 K to remove water. Pre-electrolysis was carried out in order to remove residual water and some metal impurities. All experiments were performed under Ar atmosphere at 723 K. Anhydrous SmCl_3 (99.9 wt.%; High Purity Chemical Co., Ltd.) was added directly to the melts as a Sm(III) ion source.

The working electrode was a Ni plate ($5 \text{ mm} \times 20 \text{ mm} \times 0.2 \text{ mm}^2$; 99.7%, Nilaco Co., Ltd.) or a Mo plate ($5 \text{ mm} \times 20 \text{ mm} \times 0.2 \text{ mm}^2$; 99.95%, Nilaco Co., Ltd.). All working electrodes were electropolished in a 10 mol l^{-1} H_2SO_4 aqueous solution before electrochemical measurements. A vitreous carbon rod (ϕ 6 mm; Tokai Carbon Co., Ltd.) was used as a counter electrode when it was used as an anode. An Al plate ($10 \text{ mm} \times 20 \text{ mm} \times 0.2 \text{ mm}^2$; 99.2%, Nilaco Co., Ltd.) was used as a counter electrode when it was used as a cathode. The reference electrode was an Ag wire immersed in LiCl-KCl eutectic containing 1 mol% AgCl in a Pyrex tube provided with a diaphragm at the bottom. The potential of this reference electrode was calibrated with reference to that of a Li^+/Li electrode, which was prepared by electrodepositing lithium metal on Ni wire. All potentials in this paper are given with reference to this Li^+/Li electrode potential. A potentiogalvanostat (HA-501G; Hokuto Denko Corp.) and function generator (HB-105; Hokuto Denko Corp.) connected to a personal computer (PC9801DA; NEC Corp.) were used for cyclic voltammetry and chronopotentiometry.

The Sm-Ni alloy samples were prepared by galvanostatic electrolysis or potentiostatic electrolysis using the same potentiogalvanostat. Since the Sm alloys are highly oxidizable, they cannot be washed by water. Therefore, after the electrolysis, the samples were washed by 1,2-ethanediol (99.7%; Wako Pure Chemical Co., Ltd.), which scarcely reacts with the Sm alloys, to remove salts and lithium metal. These samples were analyzed by XRD (JDX-8030; JEOL Ltd.) using the Cu-K α line at 40 kV 40 mA. The XRD patterns were compared with patterns of the Sm-Ni alloys calculated by the PowderCell software [8] using the reported crystallographic data [9]. SEM and EPMA (Hitachi; S-2300) were used to measure the thickness of the alloys and the concentration profiles of Sm and Ni.

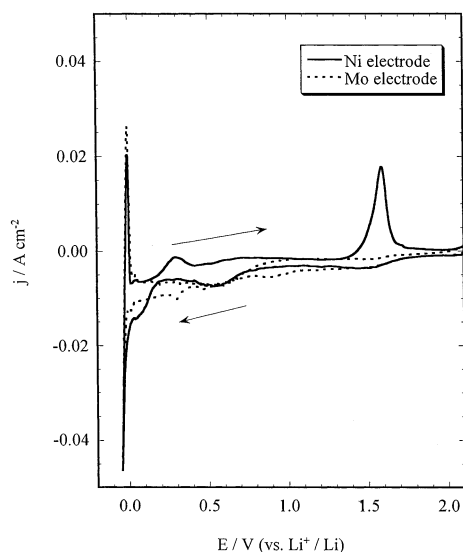


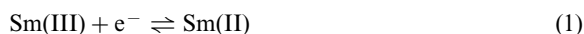
Fig. 3. Cyclic voltammograms for Ni and Mo electrodes in a molten LiCl–KCl–SmCl₃ (0.5 mol%) system at 723 K. Scan rate: 0.002 V s⁻¹.

3. Results and discussion

3.1. Cyclic voltammetry

In order to investigate Sm–Ni alloy formation, cyclic voltammetry was conducted in a molten LiCl–KCl–SmCl₃ (added 0.5 mol%) system at 723 K. The broken line in Fig. 3 shows the cyclic voltammogram of a Mo electrode at a scan rate of 0.002 V s⁻¹. The Mo

electrode was used as a reference to compare with the Ni electrode because no alloys or intermetallic compounds exist for the Mo–Sm binary system at 723 K [11]. On the cathodic sweep, cathodic currents were observed from approximately 1.60 V. They are thought to correspond to the following reaction [7].



After that, large cathodic currents were observed from 0 V, which is considered to correspond to the deposition of Li metal. After reversal of the sweep direction at -0.07 V, an anodic current peak corresponding to dissolution of the Li metal was observed.

On the other hand, the cyclic voltammogram of a Ni electrode is shown as a solid line in Fig. 3. On the cathodic sweep, cathodic currents based on reaction (1) were also observed. After that almost similar behavior to the Mo electrode was observed except the slightly larger cathodic currents at a more negative potential than 0.1 V. These cathodic currents are considered to be associated with the formation of Sm–Ni alloy. On the anodic sweep, anodic current peaks were observed at 0.29 and 1.58 V in addition to the anodic current peak of Li metal dissolution. These anodic current peaks are thought to be associated with the dissolution of Sm from the different Sm–Ni alloy phases.

3.2. Formation of Sm–Ni alloy

Based on the result of cyclic voltammetry, an alloy sample was prepared by potentiostatic electrolysis using a Ni electrode at 0.10 V for 72 h. Fig. 4 shows the XRD pattern of the surface of the sample. The observed peaks were identified as SmNi₂ and Ni substrate. However, the intensities of the Ni peaks were predominant over those of the SmNi₂ peaks, which shows that the thickness of the SmNi₂ film on the Ni substrate was very thin (estimated to be approximately 100 nm). Thus, it was found that the formation rate of SmNi₂ was very small. It is worth noting the dependence of the current on time. The cathodic current density was around 40 mA cm⁻² at the beginning. However, it decreased rapidly to about 20 mA cm⁻² in 5 min, and then reached about 10 mA cm⁻² after 1 h. It scarcely changed until the end of the electrolysis. The current density of 10 mA cm⁻² is thought to correspond mainly to current for reaction (1).

Another sample was prepared by cathodic galvanostatic electrolysis at 50 mA cm⁻² for 1 h. The electrode potential was about -0.03 V during the electrolysis. After electrolysis, the existence of liquid metal on the surface was confirmed by direct observation. This liquid metal is thought to consist mainly of lithium metal, because potassium metal does not deposit from this system and Sm metal is solid at this temperature. However, a small amount of Sm may be contained in

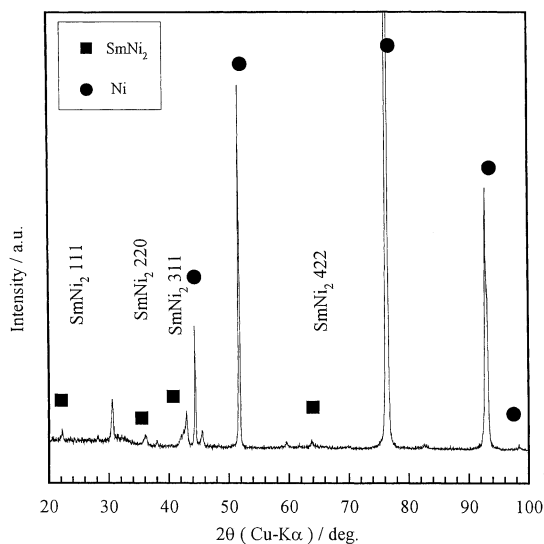


Fig. 4. XRD pattern of the Sm–Ni alloy film formed at 0.10 V for 72 h. SmNi₂: cubic unit cell with $a = 0.723$ nm. Ni: cubic unit cell with $a = 0.352$ nm.

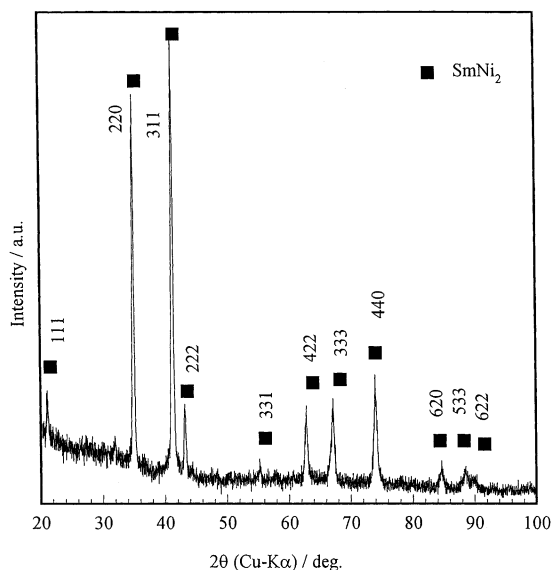


Fig. 5. XRD pattern of the Sm–Ni alloy film formed at -50 mA cm^{-2} for 1 h.

the lithium considering that the solubility of Sm in Li is around 3 atm% [10]. The XRD pattern of the sample shown in Fig. 5 was identified as SmNi_2 . The existence of Li was not observed in the XRD pattern, which can be explained by Li being removed together with the salt during the washing treatment of the electrode. Fig. 6 shows a cross-sectional SEM image and the concentration profiles of Sm and Ni by EPMA line analysis for the sample. The observed alloy layer with approximately $20 \mu\text{m}$ thickness is regarded as a uniform SmNi_2 layer, considering together with the XRD result.

From these results, it is found that the formation rate of SmNi_2 film is much larger for the latter case (cathodic galvanostatic electrolysis at 50 mA cm^{-2}) than

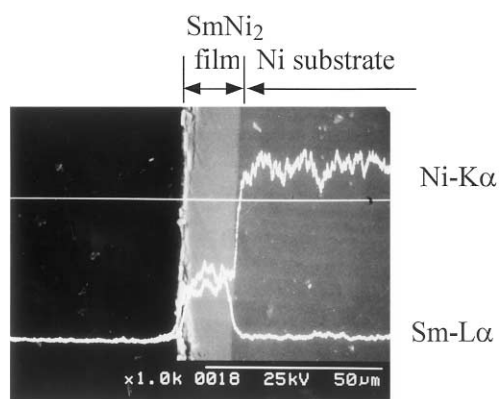


Fig. 6. Cross-sectional SEM image and concentration profiles of Sm and Ni for the sample formed at -50 mA cm^{-2} for 1 h.

the former case (potentiostatic electrolysis at 0.10 V). Since Li metal was codepositing for the latter case (cathodic galvanostatic electrolysis at 50 mA cm^{-2}) and the SmNi_2 film was rapidly formed, this electrochemical formation method was termed the ‘Li codeposition method’.

3.3. Phase control of Sm–Ni alloy film

According to the phase diagram of the Sm–Ni system (Fig. 7 [11]), there may exist eight Sm–Ni intermetallic compounds at 723 K. When Sm is dissolved anodically from an SmNi_2 electrode, there is the possibility that the SmNi_2 phase changes to other Sm–Ni alloy phases with lower Sm concentrations. In order to confirm this, chronopotentiometry was conducted for the SmNi_2 electrode at an anodic current density of 1 mA cm^{-2} . The SmNi_2 electrode was prepared by cathodic galvanostatic electrolysis at 50 mA cm^{-2} for 20 min. The obtained chronopotentiogram is shown in Fig. 8. For 1300 s in the beginning, the potential kept at 0 V, which is thought to be due to the presence of the codeposited Li metal on the electrode. After this, potential plateaus were observed at (1) 0.29, (2) 0.65 and (3) 1.20 V, respectively. These plateaus are considered to correspond to coexisting phase states of Sm–Ni alloys. Based on this result, samples were prepared by the following procedures. Firstly, SmNi_2 electrodes were made by cathodic galvanostatic electrolysis at 50 mA cm^{-2} for 1 h (Li codeposition method). Then, anodic dissolutions of Sm were conducted for 2 h by potentiostatic electrolysis at 0.1 (sample 1), 0.4 (sample 2), 0.8 (sample 3) and 1.3 V (sample 4), respectively. These potential values were determined by taking into account the potential plateaus before and after the potential jump indicating the complete phase change.

The XRD pattern of sample 1 (obtained at 0.1 V) is shown in Fig. 9. All peaks were identified as SmNi_2 , which suggests that SmNi_2 phase is stable at more negative potentials than 0.29 V.

Fig. 10 shows the XRD pattern of sample 2 (obtained at 0.4 V). It was found that the SmNi_2 phase changed completely to an SmNi_3 phase. Therefore, the potential plateau at 0.29 V is considered to correspond to the following reaction:

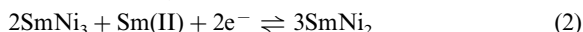


Fig. 11 shows the cross-sectional SEM image and the concentration profiles of Sm and Ni for sample 2. The thickness of the alloy layer was approximately $20 \mu\text{m}$. Since the original SmNi_2 layer had about $20 \mu\text{m}$ thickness, it changed little during phase transformation from SmNi_2 to SmNi_3 .

The XRD pattern shown in Fig. 12 identified sample 3 (obtained at 0.8 V) as SmNi_5 . Thus, the potential plateau at 0.65 V is considered to be due to the following reaction:

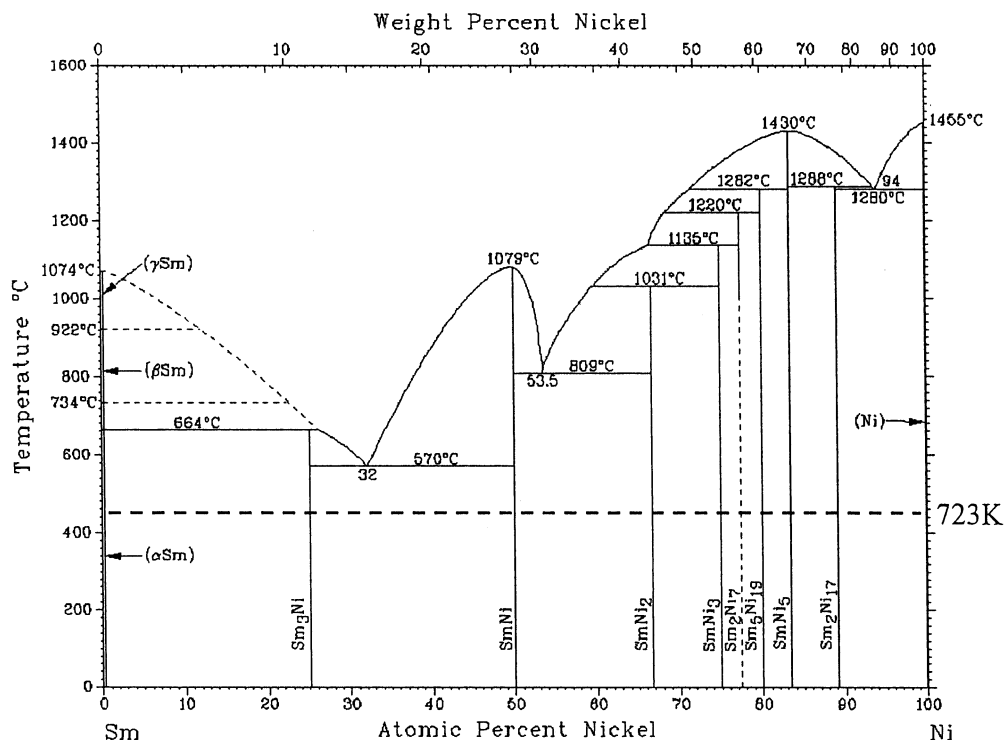
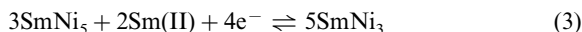


Fig. 7. Phase diagram of the Sm–Ni system [11].



According to the cross-sectional SEM image and the EPMA line analysis for sample 3 (Fig. 13), the thickness of alloy layer was approximately 20 μm .

The XRD pattern of sample 4 (obtained at 1.30 V) is shown in Fig. 14, in which only the pattern of α -Ni was observed. Accordingly, the potential plateau at 1.20 V is regarded to correspond to the following reaction:



Fig. 15 shows the cross-sectional SEM image and the concentration profiles of Sm and Ni for sample 4. From the EPMA line analysis, it was found that no Sm existed in the film.

Additionally, samples were prepared from SmNi_2 electrodes at 0.30, 0.50, 0.70 and 1.00 V, respectively, for 2 h. XRD analysis of the samples showed that SmNi_3 was formed at 0.30 and 0.50 V, and that SmNi_5 formed at 0.70 and 1.00 V. These results are consistent with the speculated reactions (2)–(4) and the estimated corresponding potentials. The above experimental results can be summarized as in Table 1. Accordingly, formation reactions of Sm–Ni alloys and the corresponding potentials were clarified as is summarized in Table 2. On the other hand, the phase diagram of the Sm–Ni system shown in Fig. 7 suggests the possibility of formation of Sm_2Ni_7 , $\text{Sm}_5\text{Ni}_{19}$ and $\text{Sm}_2\text{Ni}_{17}$. How-

ever, they were not identified in any samples under our experimental conditions. This might be explained by the fact that the formation rates of these alloys were very low.

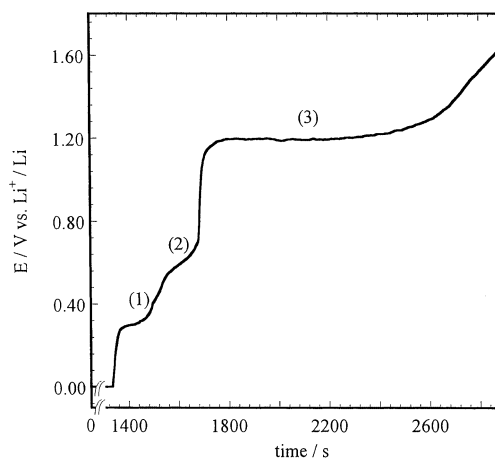


Fig. 8. Chronopotentiogram for the SmNi_2 electrode at 1 mA cm^{-2} in a molten LiCl-KCl-SmCl_3 (0.5 mol %) system at 723 K. The SmNi_2 electrode was prepared by cathodic galvanostatic electrolysis of a Ni electrode at 50 mA cm^{-2} for 20 min.

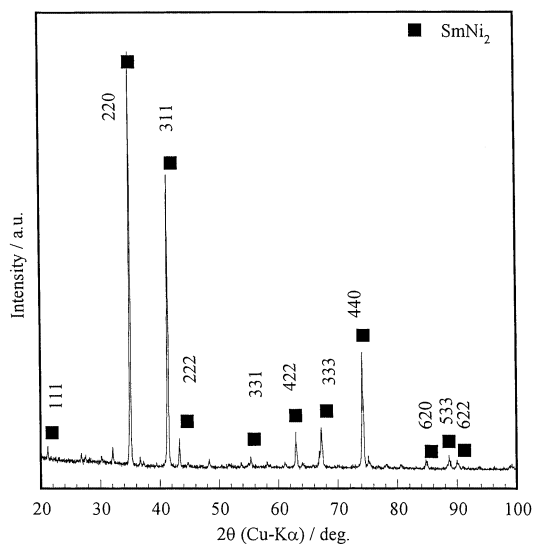


Fig. 9. XRD pattern of sample 1 prepared by anodic electrolysis of the SmNi_2 electrode at 0.1 V for 2 h. The SmNi_2 electrode was prepared by cathodic galvanostatic electrolysis of a Ni electrode at -50 mA cm^{-2} for 1 h.

4. Conclusions

Electrochemical formation of Sm–Ni alloys was studied in a molten LiCl-KCl-SmCl_3 (0.5 mol%) system at 723 K. The results obtained through this study can be summarized as follows.

The cyclic voltammogram for a Mo electrode showed the reduction wave from Sm(III) to Sm(II) at 1.60 V (vs

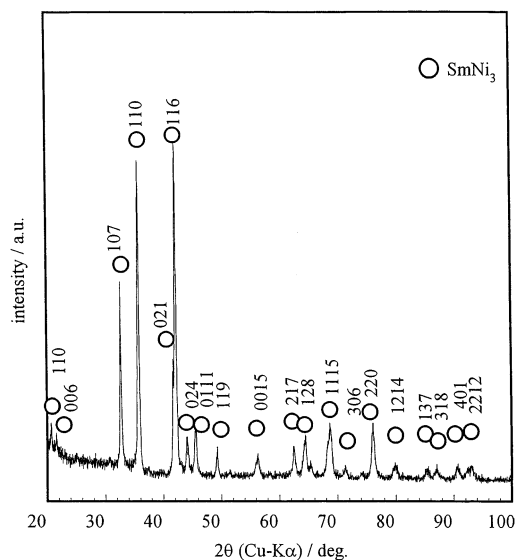


Fig. 10. XRD pattern of sample 2 prepared by anodic electrolysis of the SmNi_3 electrode at 0.4 V for 2 h. SmNi_3 ; hexagonal unit cell with $a = 0.501 \text{ nm}$, $c = 2.46 \text{ nm}$.

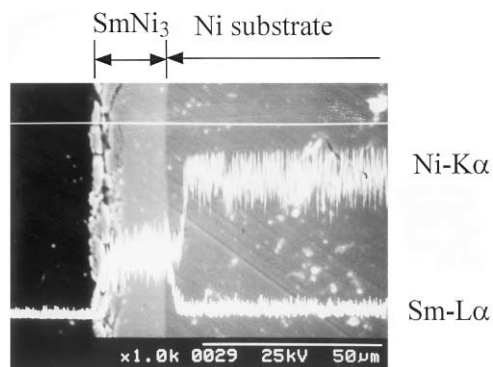


Fig. 11. Cross-sectional SEM image and concentration profiles of Sm and Ni for sample 2.

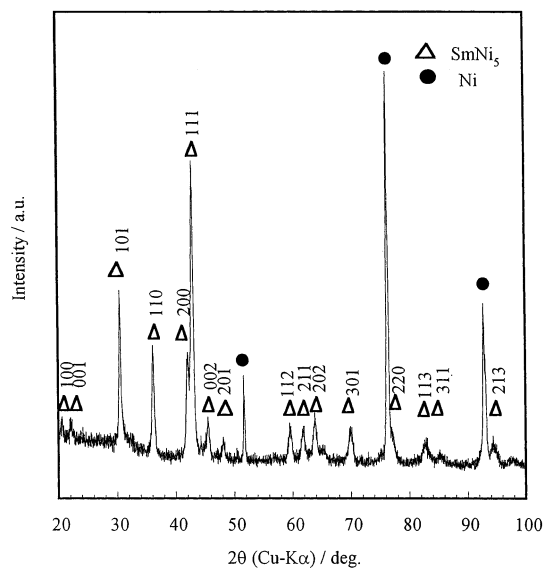


Fig. 12. XRD pattern of sample 3 prepared by anodic electrolysis of the SmNi_5 electrode at 0.8 V for 2 h. SmNi_5 ; hexagonal unit cell with $a = 0.493 \text{ nm}$, $c = 0.396 \text{ nm}$.

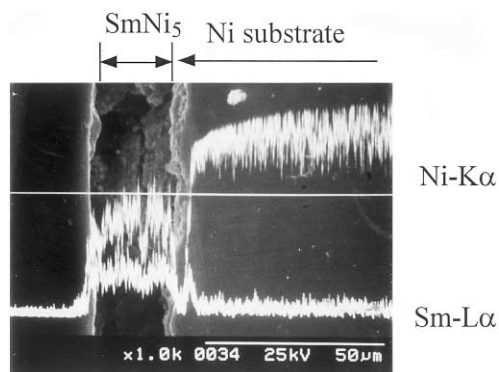


Fig. 13. Cross-sectional SEM image and concentration profiles of Sm and Ni for sample 3.

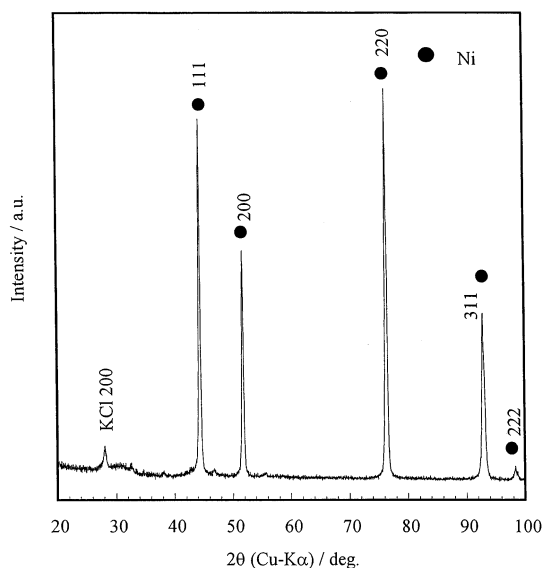


Fig. 14. XRD pattern of sample 4 prepared by anodic electrolysis of the SmNi_2 electrode at 1.3 V for 2 h.

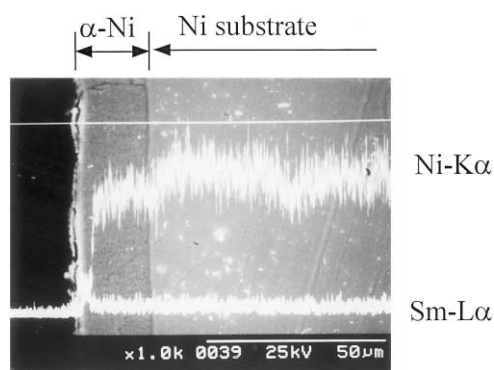


Fig. 15. Cross-sectional SEM image and concentration profiles of Sm and Ni for sample 4.

Table 1

Potentials and the identified phases for the samples prepared by potentiostatic electrolysis of the SmNi_2 electrodes for 2 h in a LiCl-KCl-SmCl_3 (0.5 mol %) system at 723 K

| Potential/V vs. Li^+/Li | Identified phase |
|---|--------------------|
| 0.10 | SmNi_2 |
| 0.30 | SmNi_3 |
| 0.40 | SmNi_3 |
| 0.50 | SmNi_3 |
| 0.70 | SmNi_5 |
| 0.80 | SmNi_5 |
| 1.00 | SmNi_5 |
| 1.30 | $\alpha\text{-Ni}$ |

Table 2

Formation reactions and the corresponding potentials for the Sm-Ni alloys in a molten LiCl-KCl-SmCl_3 (0.5 mol%) system at 723 K

| Reaction | Potential/V vs. Li^+/Li |
|--|---|
| $2\text{SmNi}_3 + \text{Sm(II)} + 2\text{e}^- \rightleftharpoons 3\text{SmNi}_2$ | 0.29 |
| $3\text{SmNi}_5 + 2\text{Sm(II)} + 4\text{e}^- \rightleftharpoons 5\text{SmNi}_3$ | 0.65 |
| $5\alpha\text{-Ni} + \text{Sm(II)} + 2\text{e}^- \rightleftharpoons \text{SmNi}_5$ | 1.20 |

Li^+/Li), but no reduction wave from Sm(II) to Sm metal. For a Ni electrode, small cathodic currents were observed at potentials more negative than 0.10 V, which indicated the formation of Sm-Ni alloy.

The formation of an SmNi_2 phase was confirmed by XRD analysis of the sample prepared at 0.10 V for 72 h. The thickness of the SmNi_2 film was estimated to be approximately 100 nm. A much thicker SmNi_2 film ($\sim 20 \mu\text{m}$) was obtained by cathodic galvanostatic electrolysis at 50 mA cm^{-2} for 1 h. Since Li metal was codepositing during the electrolysis and the SmNi_2 film was rapidly formed, the method was termed the ‘ Li codeposition method’.

In the chronopotentiogram for the SmNi_2 electrode at an anodic current density of 1 mA cm^{-2} , potential plateaus were observed at 0.29, 0.65V and 1.20 V, respectively, which were considered to correspond to coexisting phase states of Sm-Ni alloys. The SmNi_2 electrodes changed to SmNi_3 , SmNi_5 and $\alpha\text{-Ni}$ phases by anodic potentiostatic electrolysis depending on the potential. Formation reactions of Sm-Ni alloys and the corresponding potentials have been clarified.

Acknowledgements

This work was carried out with support from a Grant-in-Aid from the Japanese Ministry of Education, Science, Sports and Culture. We greatly appreciate Dr Gert Nolze for sending the PowderCell program.

References

- [1] J.M.D. Coey, *Solid State Commun.* 102 (1997) 101.
- [2] S. Yamashita, J. Yamasaki, M. Ikeda, N. Iwabuchi, *J. Appl. Phys.* 70 (1991) 6627.
- [3] G. Xie, K. Ema, Y. Ito, M.S. Zhao, *J. Appl. Electrochem.* 23 (1993) 753.
- [4] K. Tateiwa, M. Tada, Y. Ito, *Hyomen Gijutsu (J. Finishing Soc. Jpn.)* 46 (1995) 673 in Japanese.
- [5] Y. Ito, T. Nohira, *Hyomen Gijutsu (J. Finishing Soc. Jpn.)* 49 (1998) 336 in Japanese.

- [6] Y. Ito, T. Nohira, *Electrochim. Acta* 45 (2000) 2611.
- [7] K.E. Johnson, J.R. Mackenzie, *J. Electrochem. Soc.* 116 (1969) 1697.
- [8] W. Kraus, G. Nolze, *J. Appl. Crystallogr.* 29 (1996) 301.
- [9] P. Villars, L.D. Calvert, *Pearson's Handbook of Crystallographic Data for Intermetallic Phases*, ASM International, 1991.
- [10] I.N. Ganiev, A.D. Shamsiddinov, Kh.M. Nazarov, M.D. Badalov, *Metally* 4 (1996) 163 in Russian.
- [11] T.B. Massalski, J.L. Murray, L.H. Bennett, H. Baker, *Binary alloy Phase Diagrams*, American Society for Metals, 1990.